ESTABLISHING A MULTIVARIATE SPATIAL MODEL FOR URBAN GROWTH PREDICTION USING MULTI-TEMPORAL IMAGES

ABSTRACT:

Landuse change in metropolitan area has largely been focused on the dynamic nature of the urban landuse change. Few have been reported for the integrated study on both spatial and temporal change pattern in urban area. In this research, a spatial statistical model was used to support decision-making on the urban growth prediction. This model was based on the integration of remote sensing, geographical information systems and multivariate mathematical models. The emphasis of the model was on the spatial distribution of the landuse/cover units and the spatio-temporal patterns, which was modelled by landuse/cover change trajectories over a series of observation years. The main trajectories of landuse/cover change model were established based on the 5-time landuse/cover change data. Using the integrated GIS, several spatial variables were derived including proximity to the nearest road and built-up area. A multivariate model was established to model the detected urban expansion and these variables. The landuse/cover change trajectories and the multivariate model were then integrated to construct a spatial statistical model that is capable of estimating the spatial probability of the urban growth.

Introduction

Urban growth prediction is often based on the dynamic landuse/cover pattern and its relationship with selected socio-economic factors. Landuse change in metropolitan area typically reflects the economic development and population growth. Thus the analysis of spatio-temporal pattern on landuse/cover provides an objective view for the understanding of the relationship between urban growth and corresponding economic, population and environmental factors.

Research has been reported on various aspects of landuse/cover change studies (Civco *et al.* 2002). The change detection between landuse/cover categories by integrating satellite imagery, environmental and socio-economic data has been the common approach towards the analysis of the dynamic pattern of urban growth (Amissah-Arthur *et al.* 2000, Roy and Tomar 2001, Masek *et al.* 2000). Markov chain and the change matrix are widely used as the tools for the dynamic pattern analysis (Lo and Shipman 1990, Boerner *et al.* 1996). However, previous research has largely been focused on the dynamic nature of the urban landuse change. Few have been reported for the integrated study on both spatial and temporal change pattern in urban area (Yeh and Li 2001).

From the point of view of urban studies, the spatial context of landuse/cover change in the urban fringe area is of particular importance since it composes critical consideration for decision-making in urban landuse (Reenberg and Fog 1995). Urban growth prediction based on objective spatio-temporal models is therefore a fundamental component for the management and planning of a metropolitan area.

In this research, a spatial statistical model was used to support decision-making on the urban growth prediction. This model was based on the integration of remote sensing, geographical information systems and multivariate mathematical models. The emphasis of the model was on the spatial distribution of the landuse/cover units and the spatio-temporal patterns, which was modelled by landuse/cover change trajectories over a series of observation years.

This paper reports the methodology for predicting spatial pattern of urban expansion by analysing landuse change trajectories and stimulating factors such as transportation lines (highways and roads). An urban expansion prediction model has been established based on the development of multivariate spatial model that considers three categories of spatial variables, namely:

1. Landuse/cover change trajectories derived by analysing multitemporal remote sensing images,
2. Proximity to transportation lines, and
3. Proximity to the existing (or established) urban centres.

Based on the multivariate spatial model, the areas with high probabilities of urban growth can be mapped so that their spatial distribution can be analysed.

Study Area and Data

This study was undertaken at Chaoyang District, one of the fastest growing districts of Beijing metropolitan area. The district is located in the eastern part of Beijing and covers an area of 455 km^2, with a population over 1.3 million – the most populous of all districts in Beijing. The majority part of the district is characterised as urban fringe with rapid urban expansion in the past two decades. Since 1978, the area of agricultural land decreased sharply – by 18.8% from 1982 to 1989 and 6.5% from 1989 to 1992. The residential and industrial land, on the other hand, increased about 28.2% from 1982 to 1989 and 14.9% from 1989 to 1992 (Cao and Cai 1993).

Landsat TM images were acquired on 2 October 1984, 21 April 1988, 6 May 1991, 28 August 1994 and 16 May 1997. In addition, the landuse map, compiled in 1991 based on field survey at the scale of 1:50,000 was used for the accuracy assessment. The master scene (1991) was geometrically corrected and registered to the landuse map, using 36 Ground Control Points (GCP) and second-order polynomial transformation with nearest neighbour resempling. The other scenes were then registered to the master scene by image-to-image registration.

Methodology

The methodology that we employed for this study is composed of three components, namely:

- <u>Landuse/cover change trajectory analysis</u> which derives the probability of landuse transformation from various landuse categories to urban landuse,
- <u>Spatial proximity analysis</u> which derives the probability of urban growth in relation to distance to transportation and existing built-up areas, and
- <u>Establishment of multivariate spatial model to predict urban growth</u> which integrates the above derived variables to derive overall probability of urban expansion for each given location in the study area.

Landuse/cover change trajectory analysis

A time series of remote sensing images (Landsat TM), spanning 17 years were used to get landuse change information, by employing post-classification comparison technique (Lillesand and Kiefer, 2000).

Landuse classification: Two classifiers were tested in this study, namely, the *maximum likelihood* (MLC) and *artificial neural network* (NNC) classifiers. One major difference between the two classifiers is the number and purity requirement on the training areas (Atkinson and Tatnall 1997, Kanellopoulos and Wilkinson 1997). The NNC needs fewer and less pure seeding data in comparison to that of MLC.

PCI 6.0 remote sensing image processing software was used for the classification. 4835 pixels were selected as the training data on the 1991 TM image. The BP model of NNC was applied in the classification, with a structure of 6, 32 and 7 that refers to input, nods number and output, respectively. After classification, the post process was applied to both results from MLC and NNC to aggregate classified categories in order to match those of the landuse map. Five land-cover classes were mapped, namely, water, vegetable garden, forest, farmland, and built-up area.

The one-time classification error matrix was constructed for the land-cover classification on the 1991 image with the 1991 landuse map as the reference data. With an overall accuracy of 79.6% (3% higher than that of MLC) and a kappa coefficient of 0.696, NNC was chosen as the preferred classifier. The rest four multitemporal images were then classified using NNC. Together with the 1991 images, the five multitemporal classified images were used to establish the land-cover change trajectory for each pixel from 1984 to 1997.

Landuse change analysis: Changes in landuse between the successive dates were detected by post-classification comparison. The post-classification comparison leads to a categorical map that indicates the landuse classes at the two successive observation years for every pixel. The traditional post-classification cross-tabulation (Lunetta and Elvidge 1999) was employed to establish “from” and “to” categories of the two dates of the images, which was essential for the definition of landuse change trajectories.

Trajectories of landuse change: The spatio-temporal landuse shifting pattern has been an active research field of landuse change detection (Roy and Tomar 2001, Weng 2001). From the point of view of change detection, the change trajectory was defined as trends over time among the relationships between the factors that shape the changing nature of human-environment relations and their effects within a particular region (Kasperson *et al.* 1995). The trajectory of land-cover change refers to successions of land-cover types for a given sampling unit over more than two observations (Mertens and Lambin 2000, Petit *et al.* 2001). Markov chain and the change matrix could be used to analyse the possibility of landuse shift and to definite the trajectories, but they would not be applicable to get the real trajectory of a given location when the observation time series becomes long. To establish the trajectory of landuse change, we have selected numerous sample points over the study area and recorded for each sample point the landuse category at every image date.

In urban fringe area, the primary landuse change is urban growth. Among all possible landuse change trajectories, the sequences were focused on the other landuse categories turning into built-up area at the end of monitor period.

The popularity of various landuse change trajectories determines the probabilities of transforming to built-up areas from other landuse categories. The spatial variable is defined as cover type conversion probability (*C*) and used to describe spatial pattern of urban expansion in the multivariate spatial model for urban expansion prediction.

Spatial proximity analysis

Spatial proximity analysis derives the probability of urban growth in relation to distance to transportation and existing urban centers. In this study, we have utilized two categories of variables for the proximity analysis, namely, the distance between urban expansion areas to transportation lines and to existing built-up areas.

<u>The distance between urban expansion areas to transportation lines</u>: In order to analyze the influence of the transportation lines (e.g. highways) on the urban expansion, we set the variables *Kn* and *Ks*, which specify the relationship between transportation and urban expansion area by number count and area, respectively. To compute *K*, we firstly created a series of buffer zones to the transportation lines ranging from 50m, with an increment of 50m, to the maximum increments *m* (in this study we set m = 10). The variable *K* for *i*th buffer zone (e.g. i = 1 means the first 50m buffer and i = 2 means the second 100m buffer) can then be derived as:

$$Kn_i = \frac{n_i}{N} \times 100\% \qquad i = 1, 2, \ldots, m \qquad (1)$$

and $$Ks_i = \frac{s_i}{S} \times 100\% \qquad (2)$$

where *n* and *s* denote the number count and area of urban expansion areas (i.e. "clumps" of pixels identified as shifted from other landuse types to "built-up area"), and *N* and *S* denote the total number count and area of urban expansion areas in one observation period, respectively.

<u>The distance between urban expansion areas to existing built-up areas</u>: The variable *Ka* was defined to describe the proximity of the urban expansion areas to existing built-up areas that could be considered as the urban growth origins (e.g. old city). Buffer zones were created from 100m with an incremental distance of 25m to the existing built-up areas. The variable *Ka* can then be computed in the similar way as above:

$$Ka_i = \frac{a_i}{S} \times 100\% \qquad i = 1, 2, \ldots, m \qquad (3)$$

where a_i denotes the expansion area within the *i*th buffer zone to the existing built-up areas.

The incremental change within each buffer zone can be computed as:

$$\Delta K_i = K_{i+1} - K_i, \qquad i = 1, 2, \ldots, m-1 \qquad (4)$$

where ΔK_i denotes the change of K (Kn, Ks or Ka) within the ith incremental buffer zone.

During a given monitoring period t, there is D_t, which is defined as the buffer width with the maximum ΔK_i value. The D_t identifies the zone where the urban growth is most likely to happen at the given period, while ΔK_i defines the probability of urban growth for the ith buffer zone.

Establishment of multivariate spatial model to predict urban growth

The multivariate spatial model integrates various spatial variables to derive overall probability of urban expansion for each given location in the study area. It is based on four spatial variables: the above Kn, Ks and Ka, and the probability of various landuse change trajectories. The model is implemented in GIS with each spatial variable represented as a data layer. The weighting factor can then be determined by specifying given scenario based on a pre-determined urban expansion pattern (e.g. transportation dominating pattern).

To predict the spatial pattern of urban growth, the above multivariate model is applied to derive landuse transformation index to "built-up area" at a given location. The variables were weighted based on their influence on urban growth and they were then overlaid to derive the weighted sum at a given location. The result was then classified into classes to produce the map showing the likelihood of urban growth for the urban fringe region. The urban growth index (P) can be expressed as:

$$P = \frac{w_c C + w_n Kn + w_s Ks + w_a Ka}{\sum w} \qquad (5)$$

Where w denotes the weighting factor applied to a given variable.

Results and discussion

Landuse change analysis

During the entire study period from 1984 to 1997, the built-up area expanded from 26.7% to 55.9% of the total district – doubled in 14 years. On the other hand, the proportion of farmland and vegetable garden decreased from 51.1% and 15.5% to 26.3% and 6.7%, respectively. Forest area decreased slightly but the area of water bodies increased sharply – mainly due to the increase of commercial fish ponds in the district (table 1). By integrating the multitemporal classified images, we derived urban expansion map shown as figure 1.

(Insert Table 1 here)

(Insert Figure1 here)

The trajectories of landuse change

The trajectories of landuse change were analyzed using 3171 samples that were randomly selected over the district. Among the total samples, 939 samples indicate landuse change from other categories to built-up areas, showing 17 trajectories of landuse change. Among those trajectories, 43.7% were from vegetation garden to built-up area, 52.6% from farmland, and 3.8% from water (Table 2).

(Insert Table2. here)

The proximity to the transportation lines

Table 3 and table 4 show the results of ΔK_i calculated by urban expansion number and area respectively. Considering the number of newly converted built-up area, D_t shifted from the range of 150-200m to 50-100m in late 1980's. While considering the area, it continued shifting from close range of 50-100m to 250-300m (the bold numbers in the tables are the maximum ΔK_i for each period). By observing the tables, it appears that differences of ΔK_i between buffer zones were not great until the distance reached beyond 350m. There was also a tendency that proximity to transportation played a less important role than it was at early stage (e.g. 1984-1988). The normalised ΔK_i values were computed for input to Equation 5.

(Insert Table 3 here)

(Insert Table 4 here)

The proximity to the existing built-up areas

ΔKa for each buffer zone was computed in the same way as that for ΔK_i and then the Ka value for each township was also computed using area weighted ΔKa values within the township. The result shows that D_t for Ka occurred in the 125m buffer zone (figure 2), in which all townships yielded Ka greater than 60% with a majority of greater than 80% (table 5). This clearly shows the strong trend that urban growth of the District most likely occurred next to the existing built-up areas. The spatial distribution of Ka also demonstrated the tendency showing that higher growth rate tends to be associate with townships with closer proximity to the city center (figure 2).

(Insert Table 5 here)

(Insert Figure 2 here)

(Insert Figure 3 here)

Urban growth prediction

In this study, the urban growth index (P) has been computed with all weighting coefficients set to 1 (i.e. $w_c = w_n = w_s = w_a = 1$). In order to assess the prediction result, we have tested the model on 1984 image to predict urban growth probability. The resulting P values were then classified into three classes by selecting threshold values. On the 1988 landuse classification, the prediction results were tested showing that 100% Class I areas were transformed to built-up areas, and most of Class II areas were transformed as well, except the south part of the region (e.g. Xiao Hong Men township). For most Class III areas, the landuse categories were not transformed, except some farmlands in outskirt of the urban fringe region.

Based on the findings of the test, we have processed data using 1997 image and computed the P value. The result has been classified using the threshold P values of < 50%, 50 – 60% and > 60% corresponding to Class I, II and III shown on the urban growth prediction map (figure 4), respectively. Figure 4 shows the probability classes of urban expansion, on which the spatial pattern of the influence by existing built-up areas and major transportation lines has clearly shown. We predict that Class I areas would be most likely to be transformed into built-up area prior to the areas of other two classes and the rest unclassified area, though Class II areas might also present likelihood for such transformation.

(Insert Figure 4 here)

Conclusion

In this study, we have developed a multivariate spatial model, which integrates spatial variables including landuse trajectory, proximity to transportation lines and existing built-up areas, to assess the probability of urban growth indicated by the land cover transformation to built-up areas. This allows prediction of future urban growth in the urban fringe region so that to assist decision making for the management of such region.

The case study was undertaken in Chaoyang District of Beijing. Landsat TM images acquired in the years of 1984, 1988, 1991, 1994 and 1997 were used for change detection during the study period from 1984 to 1997 using of post-classification comparison method. The main trajectories of landuse change model were established based on these 5-time landuse data. There were 17 trajectories of landuse change related to the transformation to built-up area. Among the trajectories, 43.7% were transformed from vegetation garden, 52.6% farmland, and 3.8% from water.

The urban growth prediction model was then implemented using variables including the landuse trajectory, proximity to transportation lines and built-up areas. The resulting urban growth index (*P*), which is specified as probability of landuse transformation to built-up areas, was then classified and mapped to show the areas where landuse transformation to built-up areas would most likely occur.

This study has shown a promising approach to model urban growth based on multi-temporal remotely sensed imagery. Although the accuracy of the model is yet to be proved based on more detailed accuracy analysis methods and data, and it is still questionable whether the selected spatial variables and parameters are suitable and adequate for predicting the urban growth, the study has nevertheless demonstrated a practical technical methodology which can be further fine-tuned to fit into different urban growth patterns in future applications.

Future studies will further investigate the impacts and interactions of spatial variables on urban growth patterns. Suitable methodology to quantify socio-economic factors that may also play important roles in urban growth should also be studied and adopted in the multivariate spatial model. Appropriate and practical methodologies for accuracy assessment for multi-temporal landuse change trajectory analysis should also be further studied.

Reference

Amissah-Arthur, A., Mougenot, B., and Lioreau, M., 2000, Assessing farmland dynamics and land degradation on Sahelian landscapes using remotely sensed and socioeconomic data, *International Journal of Geographical Information Science*, 14(6): 583-599.

Atkinson, P.M., and Tatnall, A.R.L., 1997, Neural networks in remote sensing, *International Journal of Remote Sensing*, 18: 699-709.

Boerner, R.E.J., DeMers, M.N., Simpson, J.W., Artigas, F.J., Silva, A., and Berns, L.A., 1996, Markov models of inertia and dynamism on two contiguous Ohio landscapes, *Geographical*

Analysis, 28(1): 56-66.

Cao, X., and Cai, X., 1993, The study of Beijing Landuse, (Beijing: Beijing Science and Technology Press) (in Chinese).

Civco, D.L., Hurd, J.D., Wilson, E.H., Song, M. and Zhang, Z., 2002, A comparison of land use and land cover change detection methods, in *Proceedings of 2002 ASPRS-ACSM Annual Conference and FIG XXII Congress*, 22-26 April, available http://clear.uconn.edu/pubs.htm.

Kanellopoulos, I. and Wilkinson, G.G., 1997, Strateties and best practice for neural network image classification, *International Journal of Remote Sensing*, 18: 711-725.

Kasperson, J.X., Kasperson, R.E., and Turner II, B.L., 1995, *Regions at Risk*, (Tokyo: United Nations University Press).

Lillesand, T.M. and Kiefer, R.W., 2000, *Remote Sensing and Image Interpretation*, John Wiley & Sons, New York.

Lo, C.P., and Shipman, R.L., 1990, A GIS approach to landuse change dynamics detection, *Photogrammetric engineering and remote sensing*, 56(11): 1483-1491.

Lunetta, R.S. and C.D. Elvidge 1999, *Remote Sensing Change Detection*, Taylor & Francis, London.

Masek, J.G., Lindsay, F.E., and Goward, S.N., 2000, Dynamics of urban growth in the Washington DC metropolitan area, 1973-1996, from Landsat observations, *International Journal of Remote Sensing*, 21(18): 3473-3486.

Mertens, B., and Lambin, E., 1999, Modelling land cover dynamics: integration of fine-scale land cover data with landscape attributes, *International Journal Of Applied Observation And Geoinformation*, 1(1): 48-52

Mertens, B., and Lambin, E.F., 2000, Land-cover-change trajectories in southern *Cameroon, Annals of the Association of American Geographers*, 90(3): 467-494.

Petit, C., Scudder, T., and Lambin, E., 2001, Quantifying processes of land-cover change by remote sensing: resettlement and rapid land-cover changes in south-eastern Zambia, *International Journal of Remote Sensing*, 22:3435-3456.

Reenberg, A., and Fog, B., 1995, The spatial pattern and dynamics of a Sahelian agro-ecosystem land use systems analysis combining household survey with georelated information, *GeoJournal*, 37(4): 489-499.

Roy, P.S., and Tomer, S., 2001 Landscape cover dynamics pattern in Maghalaya, *International Journal of Remote Sensing*, 22(18): 3813-3825.

Yeh, A.G.O, and Li, X., 2001, Measurement and monitoring of urban sprawl in a rapidly growing region using entropy, *Photogrammetric engineering and remote sensing*, 67(1):83-90.

Table 1. The percentage of landuse categories for each image acquisition date.

Image date	Built-up area	Farmland	Forest	Vegetable garden	Water
1984	26.7	51.1	3.7	15.5	3.0
1988	39.8	39.9	2.7	10.7	6.8
1991	46.0	34.9	2.7	8.2	8.2
1994	49.9	32.0	3.0	6.9	8.3
1997	55.9	26.3	2.9	6.7	8.2

Table 2. The trajectories of landuse change.

Trajectory Number	1984	1988	1991	1994	1997	%
1	Others	Others	Water	Water	→ Build	0.5
2	Others	Others	Water	→ Build	Build	1.3
3	Water	→ Build	Build	Build	Build	1.1
4	Water	Water	Water	→ Build	Build	0.9
5	Vege.	→ Build	Build	Build	Build	23.3
6	Vege.	Vege.	→ Build	Build	Build	5.2
7	Vege.	Vege.	Vege.	→ Build	Build	3.8
8	Vege.	Vege.	Vege.	Vege.	→ Build	3.4
9	Farm	Vege.	→ Build	Build	Build	2.0
10	Farm	Vege.	Vege.	→ Build	Build	1.9
11	Farm	Vege.	Vege.	Vege.	→ Build	1.1
12	Farm	Farm	Farm	Vege.	→ Build	3.0
13	Vege.	Farm	→ Build	Build	Build	1.1
14	Farm	→ Build	Build	Build	Build	27.7
15	Farm	Farm	→ Build	Build	Build	6.6
16	Farm	Farm	Farm	→ Build	Build	6.4
17	Farm	Farm	Farm	Farm	→ Build	10.8

The arrow (→) symbols show when the landuse transformation has happened from other landuse types to built-up areas.

Table 3. DK_i **(by number count) values for different buffer zones to transportation lines.**

Buffer zone	1984 - 1988 ΔK_i	1984 - 1988 normalised	1988 - 1991 ΔK_i	1988 - 1991 normalised	1991 - 1994 ΔK_i	1991 - 1994 normalised	1994 - 1997 ΔK_i	1994 - 1997 normalised
50-100m	8.5	15.0	**7.8**	**13.7**	**8.6**	**15.2**	**8.4**	**14.9**
100-150m	8.3	14.7	7.2	12.6	6.8	12.1	6.2	11.0
150-200m	**8.8**	**15.6**	6.5	11.4	7.9	14.0	8.1	14.4
200-250m	5.7	10.1	7.5	13.2	6.4	11.3	8.0	14.2
250-300m	6.4	11.3	6.5	11.4	6.1	10.8	4.8	8.5
300-350m	5.8	10.3	5.8	10.2	6.9	12.2	6.9	12.3
350-400m	5.6	9.9	4.4	7.7	6.4	11.3	4.3	7.7
400-450m	4.7	8.3	6.5	11.4	4.5	8.0	5.1	9.1
450-500m	2.7	4.8	4.8	8.4	2.8	5.0	4.4	7.8
D_t (m)	150-200		50-100		50-100		50-100	

Table 4. DK_i **(by area) values for different buffer zones to transportation lines.**

Buffer zone	1984 - 1988 ΔK_i	1984 - 1988 normalised	1988 - 1991 ΔK_i	1988 - 1991 normalised	1991 - 1994 ΔK_i	1991 - 1994 normalised	1994 - 1997 ΔK_i	1994 - 1997 normalised
50-100m	**10.2**	**18.0**	5.6	10.2	6.4	11.2	7	13.4
100-150m	9.3	16.4	**8.1**	**14.8**	6.8	11.9	5.4	10.4
150-200m	8.9	15.7	4.9	8.9	8.5	14.9	4.1	7.9
200-250m	3.7	6.5	7.3	13.3	6.9	12.1	6.2	11.9
250-300m	7.3	12.9	5.6	10.2	**11.4**	**20.0**	**9.1**	**17.5**
300-350m	4.8	8.5	7.4	13.5	5.3	9.3	7.9	15.2
350-400m	5.2	9.2	3.5	6.4	5	8.8	4.3	8.3
400-450m	4.7	8.3	8.1	14.8	3.9	6.8	4.5	8.6
450-500m	2.6	4.6	4.4	8.0	2.8	4.9	3.6	6.9
D_t (m)	50-100		100-150		250-300		250-300	

Table 5. K_a **values for each township at 125m (**D_t **value) buffer zone to existing built-up areas.**

Township	1984 - 1988	1988 - 1991	1991 - 1994	1994 - 1997
Xiao Hong Men	71.8	77.8	87.0	81.0
Shi Bali Dian	75.5	90.1	100.0	93.1
Nan Muo Fang	91.5	95.8	96.9	100.0
Wang Si Ying	91.8	89.3	97.1	94.7
Gao Bei Dian	87.5	91.2	100.0	97.7
Jiang Tai	65.2	92.9	96.4	90.6
Ping Fang	73.7	87.7	94.7	96.2
Dong Ba	38.6	86.3	94.4	88.5
Lou Zi Zhuang	47.4	58.8	73.0	82.4
Jing Zhan	41.7	36.6	85.0	66.7
Lai Guang Ying	76.7	93.4	89.5	81.1
Tai Yang Gong	96.9	92.3	100.0	100.0
Da Tun	82.8	87.5	100.0	93.8
Wa Li	68.4	84.8	100.0	91.8
Shuang Qing	78.7	89.9	92.8	94.3
Dong Ba	46.7	72.1	76.7	72.1
Dong Feng	87.2	90.0	95.5	96.9
Average	**71.9**	**83.3**	**92.9**	**89.4**

Figure Captions

Figure.1. Urban expansion map from 1984 to 1997.

Figure 2. *Ka* values decrease with increasing distance to built-up areas.

Figure 3. Distribution of *Ka* within 125m buffer zone in Chaoyang District of Beijing (1997).

Figure 4. The map of probability of urban growth prediction (1984).

Figure.1.

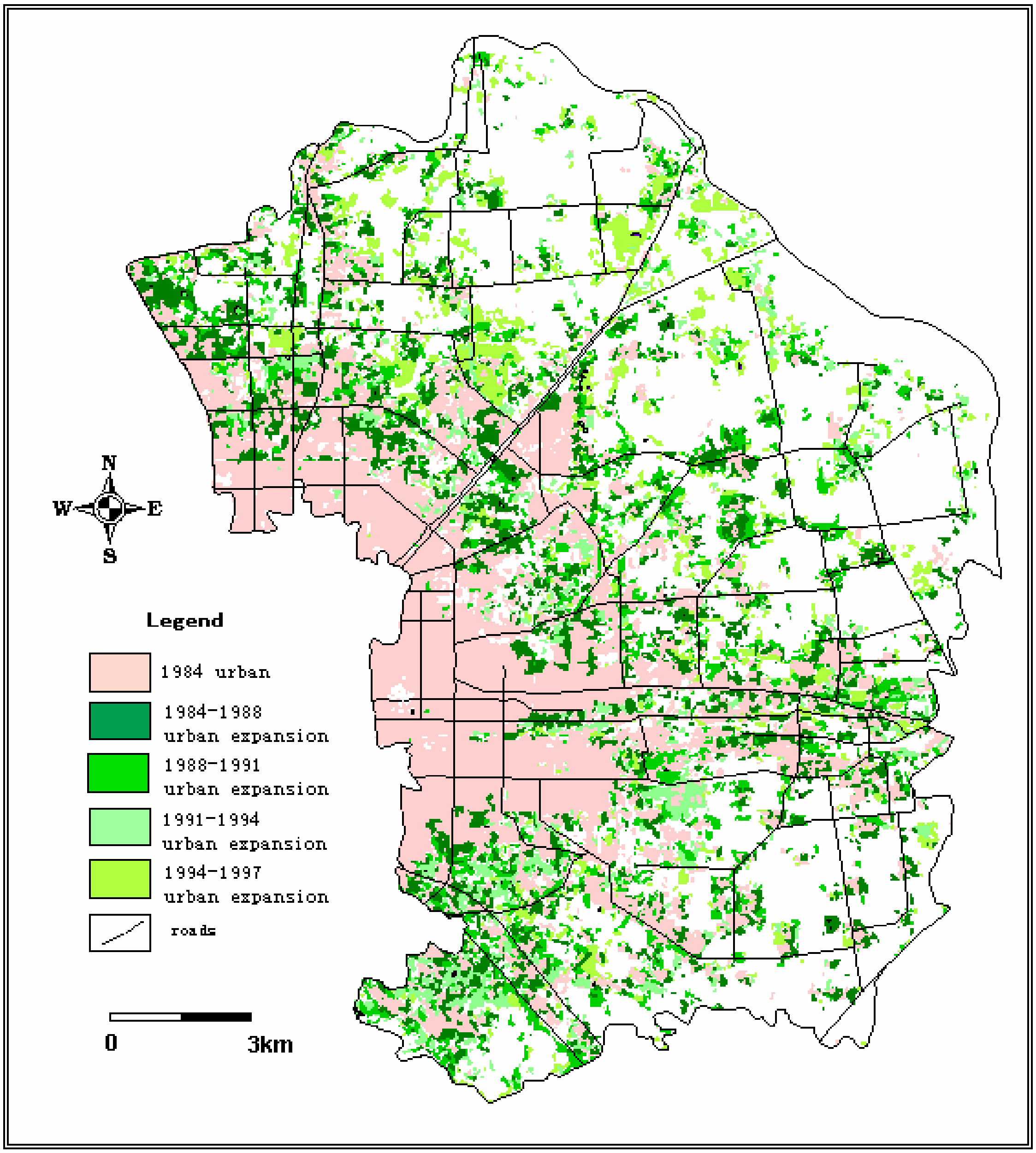
N
W
E
S
Legend
1984 urban
1984-1988
urban expansion
1988-1991
urban expansion
1991-1994
urban expansion
1994-1997
urban expansion
roads
0
3km

Figure 2.

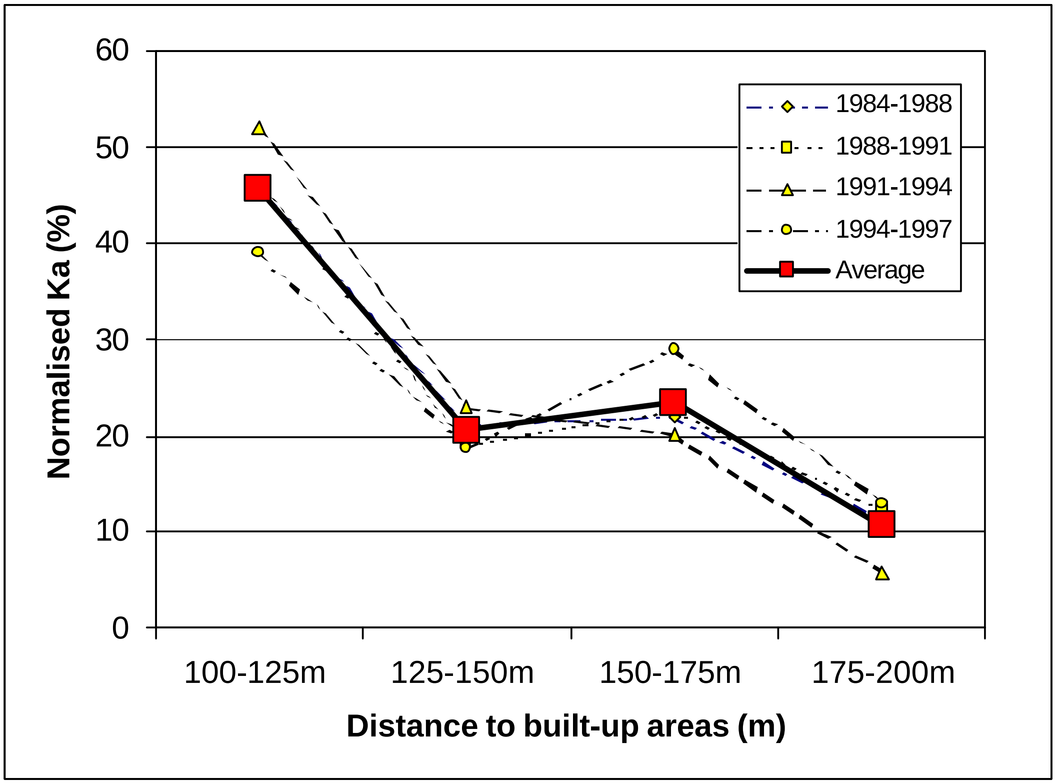

60
50
40
30
20
10
0
Normalised Ka (%)
1984-1988
1988-1991
1991-1994
1994-1997
Average
100-125m
125-150m
150-175m
175-200m
Distance to built-up areas (m)

Figure 3

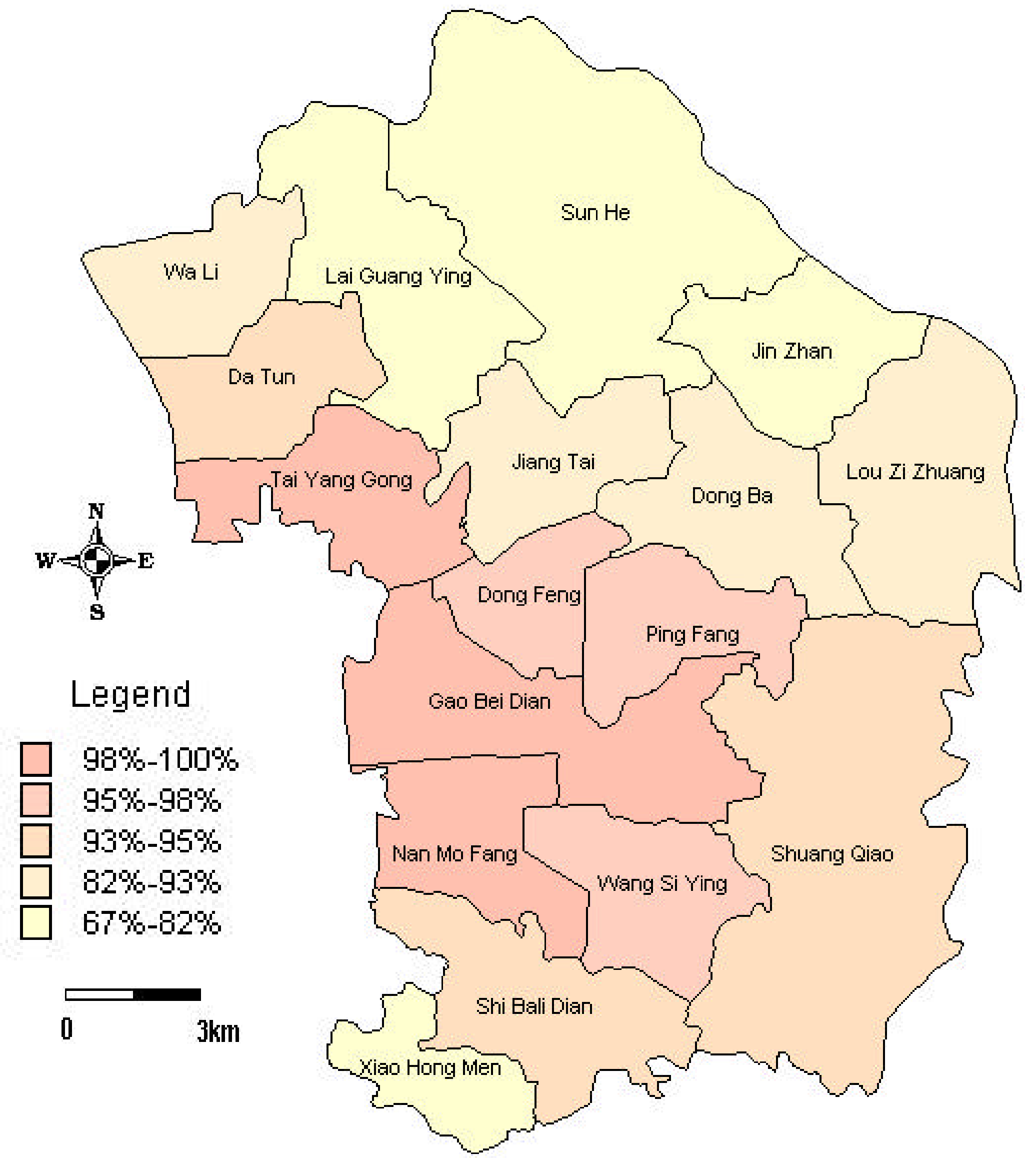
Sun He
Wa Li
Lai Guang Ying
Jin Zhan
Da Tun
Lou Zi Zhuang
Jiang Tai
Tai Yang Gong
Dong Ba
N
W
E
S
Dong Feng
Ping Fang
Legend
Gao Bei Dian
98%-100%
95%-98%
93%-95%
Nan Mo Fang
Shuang Qiao
82%-93%
Wang Si Ying
67%-82%
0
3km
Shi Bali Dian
Xiao Hong Men

Figure 4.